Theor Chem Acc (2007) 118:89–97
DOI 10.1007/s00214-007-0247-0

REGULAR ARTICLE

Magnetotropicity of phosphole and its arsenic analogue

Stefano Pelloni · Paolo Lazzeretti

Received: 21 November 2006 / Accepted: 13 December 2006 / Published online: 1 February 2007

Abstract Spatial ring current models for the phosphole molecule and its arsenic parent have been constructed. Diatropism of these molecules is quite peculiar and fundamentally different from that of benzene as shown by stagnation graphs of current density field. Maps of shielding density are helpful for interpreting the effect of electronic currents on nuclear shielding. Constrained planarity increases the degree of diatropicity quantitatively specified by magnetic descriptors, which implies that ring currents go together with π-electron distortivity.

1 Introduction

The meaning of expressions like "aromatic character" or "aromatic behaviour" is quite vague despite their current use in the chemical literature. On the one hand, the word "aromaticity" seems to connote a commonly accepted idea, or even an essential category of the chemical thinking, on the other, no simple and indisputable definition has so far been provided in rigorous quantum mechanical terms.

"Aromaticity indicators" that should help understand this elusive quality are frequently proposed [1]. There is also a general consensus that aromaticity can be "measured" by geometric, energetic, and magnetic quantifiers. However, extended analyses proved that widely employed descriptors "do not speak with the same voice" and that "the phenomenon of aromaticity is regarded as statistically multidimensional" [2]. Nonetheless, several studies indicate that different aromaticity measures may collide, providing divergent information. For instance, the most stable fused heterobicycles are not the most aromatic positional isomers [3].

Non disputable, agreed definitions of aromaticity should be arrived at in terms of measurable molecular properties [4], therefore magnetic response appears to offer most reliable criteria. Investigations on bisheteropentalenes $C_6H_4X_2$ showed that the [3,4c] isomer is the least stable, but most diatropic, compound for X = NH, O, S, and PH [5–8]. Analogously, stronger diatropicity is apparently compatible with smaller energetic stabilisation in tetraazanaphthalenes [9]. We can possibly claim that the word aromaticity does not convey a generally accepted semantic value, despite its frequent use. Therefore, throughout this paper, "aromaticity" will be used as a colloquial term, whereas "magnetotropicity" is assumed to stand on more firm ground, as it can be related to experimentally accessible quantities, say, magnetic susceptibility and nuclear magnetic shielding.

2 Aromaticity of heterocyclic pentatomics containing phosphorous and arsenic

The aromaticity of planar phosphole and its arsenic analogue – both saddle points of the inversion motion – is significantly larger than that of the non planar structures corresponding to the minimum on the energy hypersurface. This has early been established for phosphole by Mislow and coworkers [10,11]. More recently, the aromaticity of the planar structure was assessed by a

Contribution to the Fernando Bernardi Memorial Issue.

S. Pelloni · P. Lazzeretti (✉)
Dipartimento di Chimica,
Università degli Studi di Modena e Reggio Emilia,
Via Campi 183, 41100 Modena, Italy
e-mail: lazzeret@unimo.it

initio calculations, adopting energetic, geometric and magnetic indicators [12–14]. Spectroscopic and chemical evidence has been reported for increased delocalisation with partially planarized [15,16] and fully planarized phosphole [17]. It is generally accepted now that the aromatic stabilisation of the planar structure is insufficient to overcome the inherently high inversion barrier at phosphorous and arsenic [18]. If planarization occurs, strong delocalisation is achieved [19].

Allowing for criteria previously outlined [20], we have chosen magnetic response properties (susceptibility, hydrogen and carbon nuclear shielding), bond lengths, and molecular energies as quantitative indicators that can be related to experimentally available information in the C_4H_4PH and C_4H_4AsH molecules. These quantities were evaluated for the bent compounds, i.e., the real molecules, denoted by I, for a partially flat geometry II (in which only the H–As and H–P bonds lie out of the plane), and fully planar structures III (Fig. 1). The magnitude of the magnetic properties for different geometries is compared and discussed in connection with salient features of the electron current density induced by a static magnetic field at right angles to the plane containing four C atoms.

A survey of model cyclic systems H_6 and Li_6 proved that only the former shows enhanced diamagnetism, possibly originating from instability of the six delocalized σ electrons [4]. Then the hypothesis that the onset of ring currents in benzene and other planar conjugated systems might be ascribed to some peculiar property of delocalized π-electrons, i.e., their intrinsic distortivity [21] and consequent instability, was advanced [4].

This is not completely unprecedented – aromatic transition states provide a clear example of the parallels between maximization of ring currents and energy increase [22,23]. However, no convincing evidence of a link between energetic instability and diatropicity has been given so far. A set of reasons in favour of this connection, which would have major consequences on our comprehension of aromaticity, is given in the present investigation of C_4H_4PH and C_4H_4AsH molecules. Some qualitative conclusions have recently been reported, indicating that the diatropicity of these

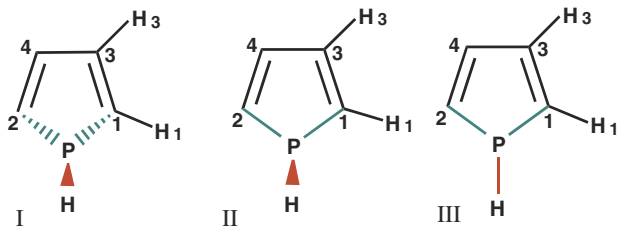

Fig. 1 Bent (I), partially flat (II), and fully planar (III) posphole molecule

nonplanar systems increases, if a constrained planar geometry is assumed [14].

3 Results and discussion

Molecular geometries have been optimised at the B3LYP/6-31++G** level of accuracy, using the GAUSSIAN98 code [24]. Magnetic properties have been calculated via the numerical DZ2 and PZ2 variants [25] of a procedure using continuous transformation of the origin of the current density-diamagnetic zero (CTOCD-DZ) and paramagnetic zero (CTOCD-PZ) [4], implemented at the Hartree-Fock level in the SYSMO package [26], employing the (13s8p/8s) substrata from van Duijneveldt for C/H [27].

The s basis for C has been augmented by a diffuse function with exponent 0.0399. The (s/p) basis set has been contracted to [9s6p/6s]. Three 3d functions, with exponents 2.1409, 0.64240, and 0.23613, and three 2p functions, with exponents 2.0731, 0.49099, and 0.15182, have been added on C and H, respectively. The (12s9p) basis for P from Ref. [28] has been augmented with six 3d functions with exponents 14.4, 4.8, 1.6, 0.4, 0.133, and 0.0433. The uncontracted (21s14p10d2f) basis from Ref. [29] was used for As. The corresponding GIAO (gauge-including atomic orbital) basis sets were employed in the DALTON [30] code to evaluate magnetic susceptibilities and nuclear magnetic shieldings. The results of the calculations are shown in Tables 1, 2 and 3.

The predictions from different approximations are virtually identical in most cases, therefore only the PZ2 nuclear magnetic shieldings are shown in the Tables. We expect that near Hartree–Fock accuracy has been attained, as indicated by closeness of DZ2, PZ2, and GIAO predictions.

According to the ring-current model (RCM) [4], the delocalized currents induced in the mobile π electrons by a magnetic field perpendicular to the four-carbon plane exalt the out-of-plane component $\chi_{\parallel} \equiv \chi_{xx}$ of the magnetic susceptibility tensor $\chi_{\alpha\beta}$, and diminish (enhance) the out-of-plane component $\sigma_{\parallel}^{H} \equiv \sigma_{xx}^{H}$ of the nuclear magnetic shielding of ring protons ($\sigma_{\parallel}^{C}$ of ring carbons) in diatropic unsaturated cyclic hydrocarbons [31,32].

The in-plane components of tensor properties are not affected by ring currents. In fact, the theoretical χ_{yy} and χ_{zz} are approximately half the value of the out-of-plane component, as can be observed in Tables 1 and 2. The σ_{yy}^{H} and σ_{zz}^{H} components are bigger than σ_{xx}^{H} for the ring hydrogen atoms H_1 and H_3. The ring currents enhance the out-of-plane component of the shielding of distant nuclei via a mechanism described in

Table 1 Magnetic susceptibility and magnetic shielding at the nuclei of C_4H_4AsH (in ppm)

Property	*xx*	*yy*	*zz*	*Av*
$\chi(DZ2)$	−919.14	−517.40	−524.72	−653.75
$\chi(PZ2)$	−940.59	−539.91	−554.61	−678.37
$\chi(GIAO)$	−960.90	−566.00	−569.04	−698.65
$\sigma^{C_1}(PZ2)$	167.46	42.44	−80.01	43.30
$\sigma^{C_3}(PZ2)$	148.14	33.96	−59.79	40.77
$\sigma^{As}(PZ2)$	1396.45	1542.22	1673.25	1537.31
$\sigma^{H_1}(PZ2)$	23.69	25.91	24.53	24.71
$\sigma^{H_3}(PZ2)$	22.28	28.44	23.03	24.58
$\sigma^{H_5}(PZ2)$	33.41	25.03	22.99	27.14

In cgs au per molecule. The conversion factor to cgs emu per mole is $a_0^3 N_A = 8.9238878 \times 10^{-2}$; for further conversion to SI units, $1\,JT^{-2} = 0.1$ cgs emu. The origin of the coordinate system lies at the centre of mass. The *x* axis is perpendicular to the plane of four carbon atoms, the heteroatom and the hydrogen bent to it lie on the xy plane bisecting the C-C bond in front of it

Table 2 Magnetic susceptibility and magnetic shielding at the nuclei of phosphole (in ppm)

Property	*xx*	*yy*	*zz*	*Av*
$\chi(DZ2)$	−893.58	−450.18	−461.17	−601.64
$\chi(PZ2)$	−891.27	−457.57	−465.59	−604.81
$\chi(GIAO)$	−899.32	−464.97	−469.87	−611.39
$\sigma^{C_1}(PZ2)$	169.73	45.43	−74.63	46.85
$\sigma^{C_3}(PZ2)$	153.60	30.44	−58.63	41.80
$\sigma^{P}(PZ2)$	367.04	383.63	463.95	404.87
$\sigma^{H_1}(PZ2)$	23.62	25.84	24.28	24.58
$\sigma^{H_3}(PZ2)$	22.16	27.99	23.18	24.44
$\sigma^{H_5}(PZ2)$	29.50	26.04	24.72	26.75

See the footnote to Table 1 for conversion factors to SI and cgs systems of units and for the coordinate system

Table 3 Parallel component of hydrogen and carbon nuclear magnetic shielding (in ppm), and of magnetic susceptibility (in ppm cgs au), C–C bond lengths (in Å), and molecular DFT(B3LYP) energies (in hartree)

Molecule	$\sigma_{\parallel}^{H1}$	$\sigma_{\parallel}^{H3}$	$\sigma_{\parallel}^{C1}$	$\sigma_{\parallel}^{C3}$	$-\chi_{\parallel}$	C_1–C_3	C_3–C_4	−Energy
C_4H_5As I	23.7	22.3	167.5	148.1	941	1.349	1.464	2388.633
C_4H_5As II	23.3	21.8	175.3	155.8	977	1.382	1.427	2388.610
C_4H_5As III	21.1	20.6	180.42	176.6	1230	1.382	1.427	2388.579
C_4H_5P I	23.6	22.2	169.7	153.6	891	1.355	1.459	495.149
C_4H_5P II	23.2	21.8	174.7	159.3	922	1.389	1.422	495.129
C_4H_5P III	21.5	20.7	179.8	178.0	1110	1.389	1.422	495.111

The field is normal to the the plane of four C atoms. See the footnote to Table 1 for conversion factors to SI and cgs systems of units and for the coordinate system

Ref. [32]. In the benzene molecule, the positive contribution of ring currents to $\sigma_{\parallel}^{C}$ amounts to ≈10%. A similar effect is expected for the carbon nuclei of C_4H_4PH and C_4H_4AsH. However, the magnitude of σ_{xx}^{C} of carbon shielding is mainly determined by local flow [33].

The magnetic descriptors quantify the diatropicity (i.e., "magnetic aromaticity") increase caused by forcing C_4H_4AsH and C_4H_4PH to be planar, as documented in Table 3.

4 Ring current model for C_4H_4PH and C_4H_4AsH

The results obtained for magnetic properties are fully explained by the RCM: the maps of the current density **J** in Fig. 2 show continuously increasing delocalisation of the electron flow from the real distorted structures I to partially and fully planar structures II and III [34]. The paramagnetic vortex about the centre of the pentatomic ring is also characteristic of aromatics [4]. Its size diminishes on increasing the planarity of the molecules.

Another quite significant feature can be observed in the maps. In the region of the formal double bonds C_1–C_3 and C_2–C_4, the current density has an out-of-plane (paramagnetic) component, which makes it to spiral outward. The portrait of a focus [4] is visible in these domains. Such a flow, typical of isolated C–C double bonds, was observed in ethylene [35] and in other pentatomic heterocyclic molecules [36]. This point was

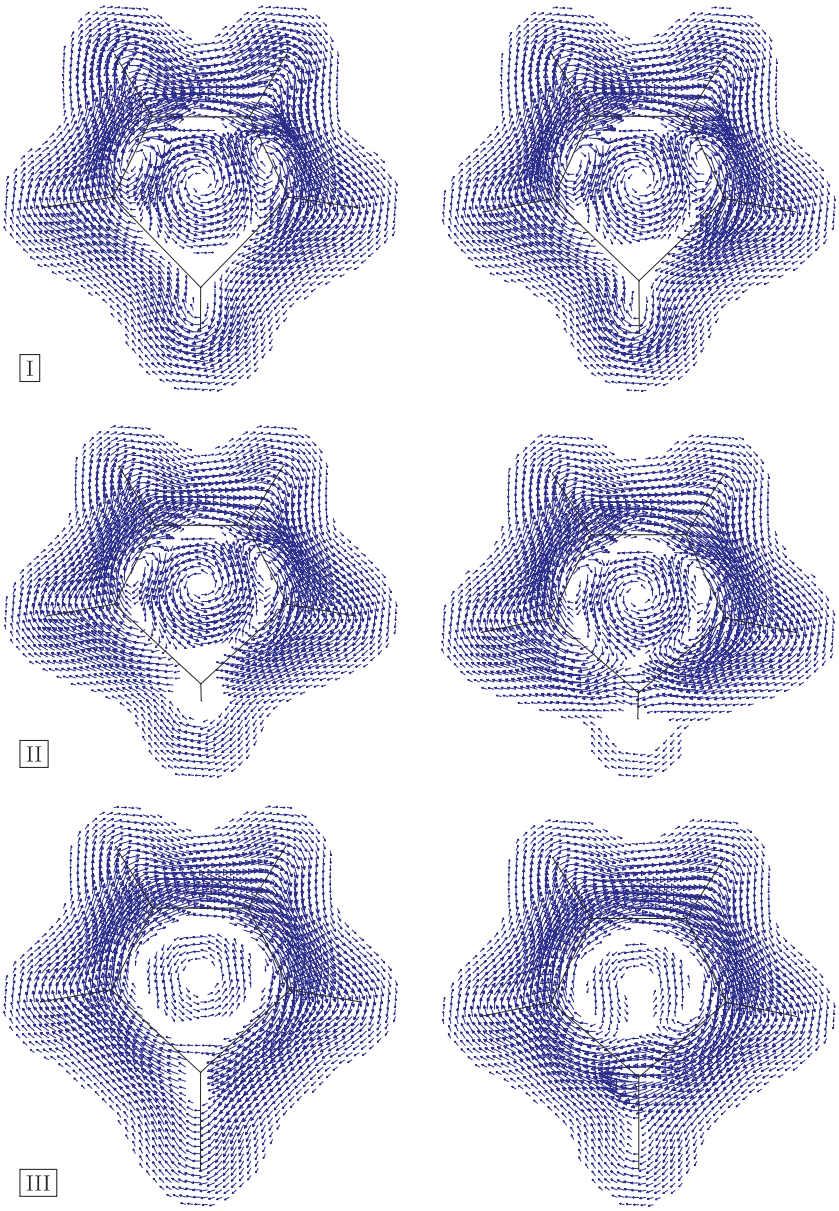

Fig. 2 Representation of the current density vector field in C_4H_4AsH (*left*) and C_4H_4PH (*right*) for geometries I, II, and III (from *top to bottom*). The length of the arrows is proportional to the intensity $|\mathbf{J}|$. The *yz* plot plane is parallel to that of four C atoms, at the distance of 1 bohr above it, on the side of the As–H and P–H bonds for I and II

not investigated by Johansson and Jusélius, compare for Fig. 4 of Ref. [14].

Diatropic planar systems, e.g. benzene and other, electrically neutral or charged, C_nH_n cyclic compounds are instead characterised by diamagnetic vortical regime over the C–C bonds [33,37]. Thus, the magnetic response of real C_4H_4PH and C_4H_4AsH molecules presents superimposed features of conjugated and non conjugated compounds.

The diatropicity of the system is controlled by its planarity: as the maps clearly show, the size of spiral flow in the vicinity of the C–C double bonds, typical of ethylene, diminishes from I to III. The maximum modulus $|\mathbf{J}|$ (in au, for a magnetic field $\mathbf{B}$ having the intensity of 1 au) increases from 7.88×10^{-2} for I and 8.60×10^{-2} for II, to 9.90×10^{-2} for III in phosphole. Corresponding values for C_4H_4AsH are 7.49×10^{-2} for I, 8.13×10^{-2} for II, and 9.82×10^{-2} for III. The contribution to $|\mathbf{J}|$ from the localised σ electron is expected to be substantially the same for the three molecular geometries. The stronger intensity $|\mathbf{J}|$ observed for flattened geometries can only be imputed to higher mobility of π electrons, connected with their distortive propensity, which is enhanced by constrained planarity [21]. Moreover, the streamline and $|\mathbf{J}|$-modulus maps [34] show clearly that, by flattening, the intensity of the current field tends to increase, becoming fairly homogeneous over the four carbon atoms of the pentatomic ring. This is another proof of the presence of quasi-uniform ring currents taking place in the flattened forms II and III.

However, the current density maps reported in Ref. [14] and in Fig. 2 are not sufficient to show the spatial aspects of the electron flow all over the molecular domain, which may cause incorrect interpretation of magnetic response properties, nuclear magnetic shielding in particular. Confusion between vortices and foci [4] often arises in the arrow representation of the current field. Sometimes similar phase portraits correspond to very different regimes.

A spatial RCM is actually needed to visualise a current density field. A stagnation graph (SG) showing the set of stagnation points (SP) and stagnation lines (SL) at which the modulus $|\mathbf{J}|$ vanishes, i.e., the electrons stop moving [38–40], provides fundamental information on the third dimension of the vector field [4,33,36]. An SG is usually a complicated topological object, and its interpretation is much facilitated by using a graphic software developed in our laboratory to obtain 3-dimensional representations that can be magnified and rotated by three Eulerian angles [34].

The SGs for C_4H_4AsH and C_4H_4PH, in a magnetic field perpendicular to the plane containing four ring carbon atoms, are shown in Figs. 3 and 4. There is a strong difference between the graphs in Figs. 3 and 4, and those reported for benzene and other C_nH_n aromatic cyclic molecules [33], which show a primary diamagnetic vortex, flowing in the tail regions of the molecular domain and splitting up into n diamagnetic vortices at

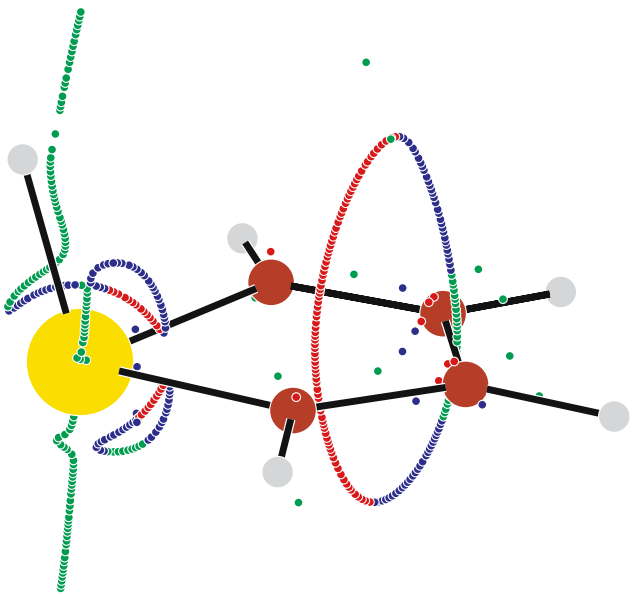

Fig. 3 Perspective view of the stagnation graph of the current density vector field in C_4H_4AsH. The uniform external magnetic field **B** is parallel to the x axis through the centre of the ring, perpendicular to the plane of the C atoms. *Green* (*red*) *lines* denote diamagnetic (paramagnetic) vortices, saddle lines are *blue*

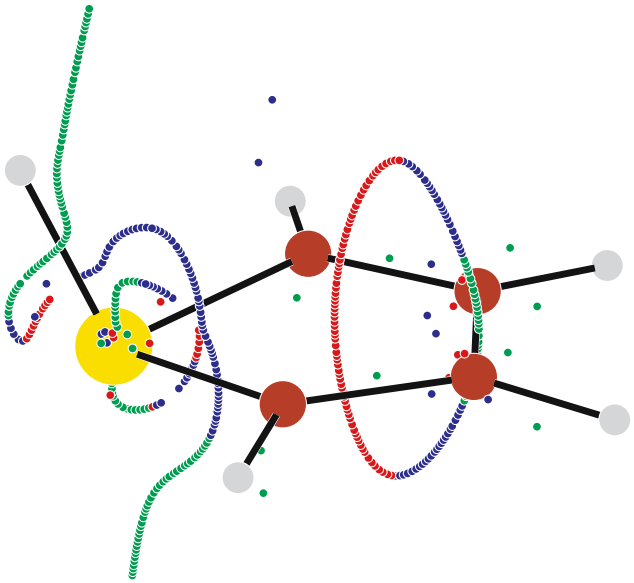

Fig. 4 Perspective view of the stagnation graph of the current density vector field in phosphole. Graphical conventions are the same as in Fig. 3

two branching points, at a distance of ≈2.5 bohr above and below the molecular plane for C_6H_6 and $C_5H_5^-$ [33]. In C_nH_n diatropic cyclic systems, branching of the primary vortical SL gives rise to n diamagnetic vortices that terminate in the region of the C–C bonds [33].

Instead, the common signature of the five-membered heterocycles is given by a closed stagnation loop, separated from the rest of the SG, passing through the midpoint of the pentagon side opposite to the heteroatom [36]. The (green) diamagnetic vortex line crossing the C-C bond and the (red) paramagnetic vortex line, flowing in the vicinity of its centre of mass, are connected by segments of (blue) saddle lines.

The SG of C_4H_4AsH and C_4H_4PH is strongly affected by constrained planarity. The closed loop is observed also in the fully planar form III. In the partially planarized form II the closed loop is replaced by an open line, with paramagnetic vortical character near the centre of mass of the molecule. Graphs for structures II and III are available [34].

The trend of streamlines and moduli is consistent with that of calculated magnetic tensor components. The diamagnetic shift of $\sigma_{\parallel}^{C}$, ≈29 (≈24) ppm from I to III in C_4H_4AsH (C_4H_4PH), and the paramagnetic shift of $\sigma_{\parallel}^{H}$, ≈1.7 (≈1.5) ppm for H_3 in C_4H_4AsH (C_4H_4PH), are explained by the differential Biot–Savart law (BSL), which gives magnitude and sign of the element of magnetic field $d\mathbf{B}_{\mathrm{ind}}$ induced on a probe [31,32,41]. Figs. 5 and 6, reporting maps of shielding density [31,32,41], help rationalise magnetic shielding at the nuclei by neatly showing molecular domains that provide negative

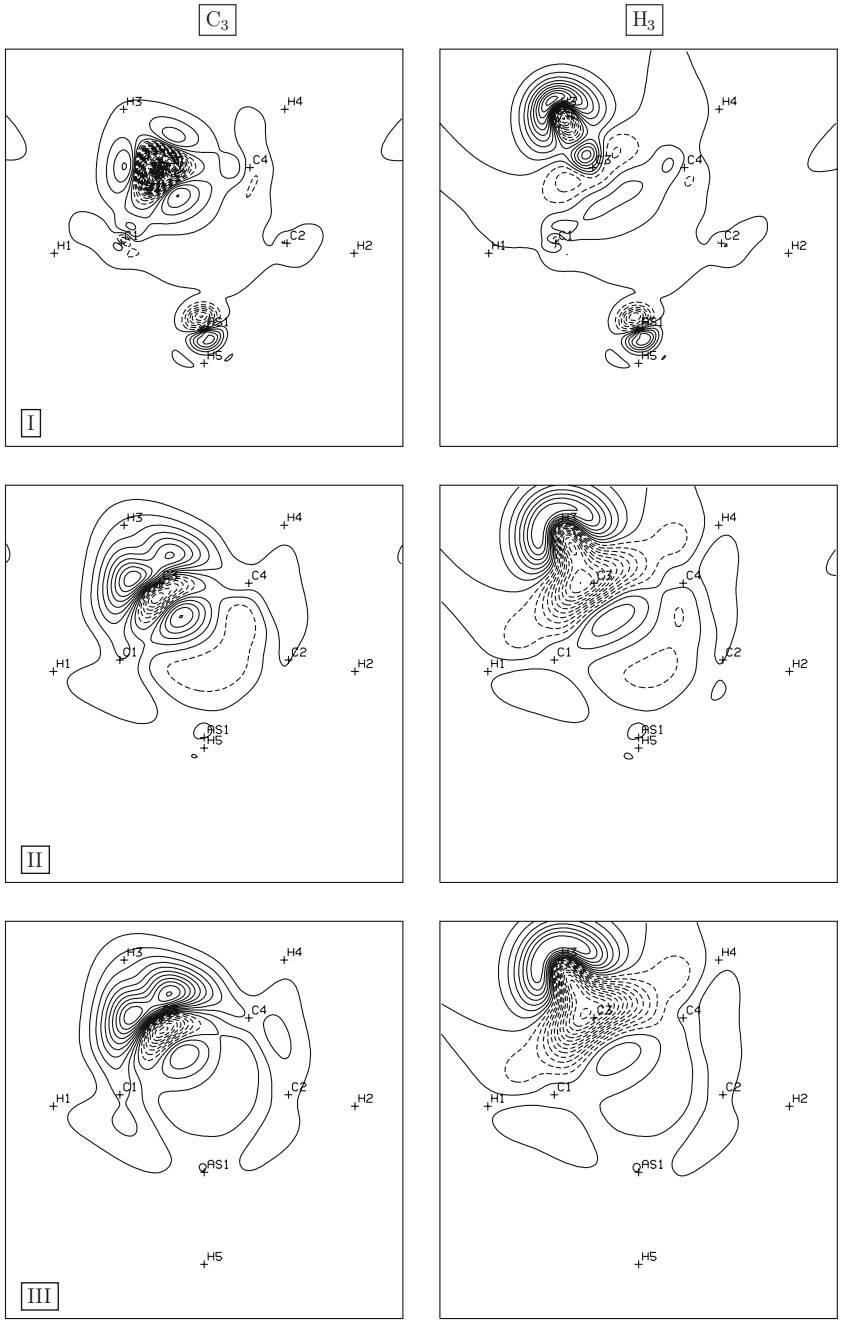

Fig. 5 The out-of-plane shielding density at hydrogen and carbon nuclei of C_4H_4AsH induced by a magnetic field in the x direction. The plot planes are the same as in Fig. 2. The contours are associated with constant magnitude and are drawn in steps of 2×10^{-3} and 1×10^{-3} au for C and H, respectively

(positive) contributions. Dotted (continuous) lines denote deshielding (shielding).

The contribution from a portion of ring current closer to a probe, e.g. a proton H outside of it, with coordinates $\mathbf{R}_H$, reinforces the external field B_x by providing a positive $dB_{\mathrm{ind},x}(\mathbf{R}_H)$, so that the σ_{xx}^H component diminishes (paramagnetic shift). On the other hand, remote portions of the circuit will induce negative contributions $dB_{\mathrm{ind},x}(\mathbf{R}_H)$, enhancing σ_{xx}^H (diamagnetic shift). Net overall deshielding, weakly cancelled by distant shielding contributions, takes place in a small domain in the proximity of the proton. A similar analysis applies to carbon shielding [31,32,41]. The maps in Figs. 5 and 6 show that the effects of ring currents increase by flattening.

Analogous indications are given by the out-of-plane component of the magnetic susceptibility. Compared to I, the increase of the diatropicity measure $|\chi_\parallel|$ in III is enormous, ≈30 and ≈25%, respectively in C_4H_4AsH and C_4H_4PH.

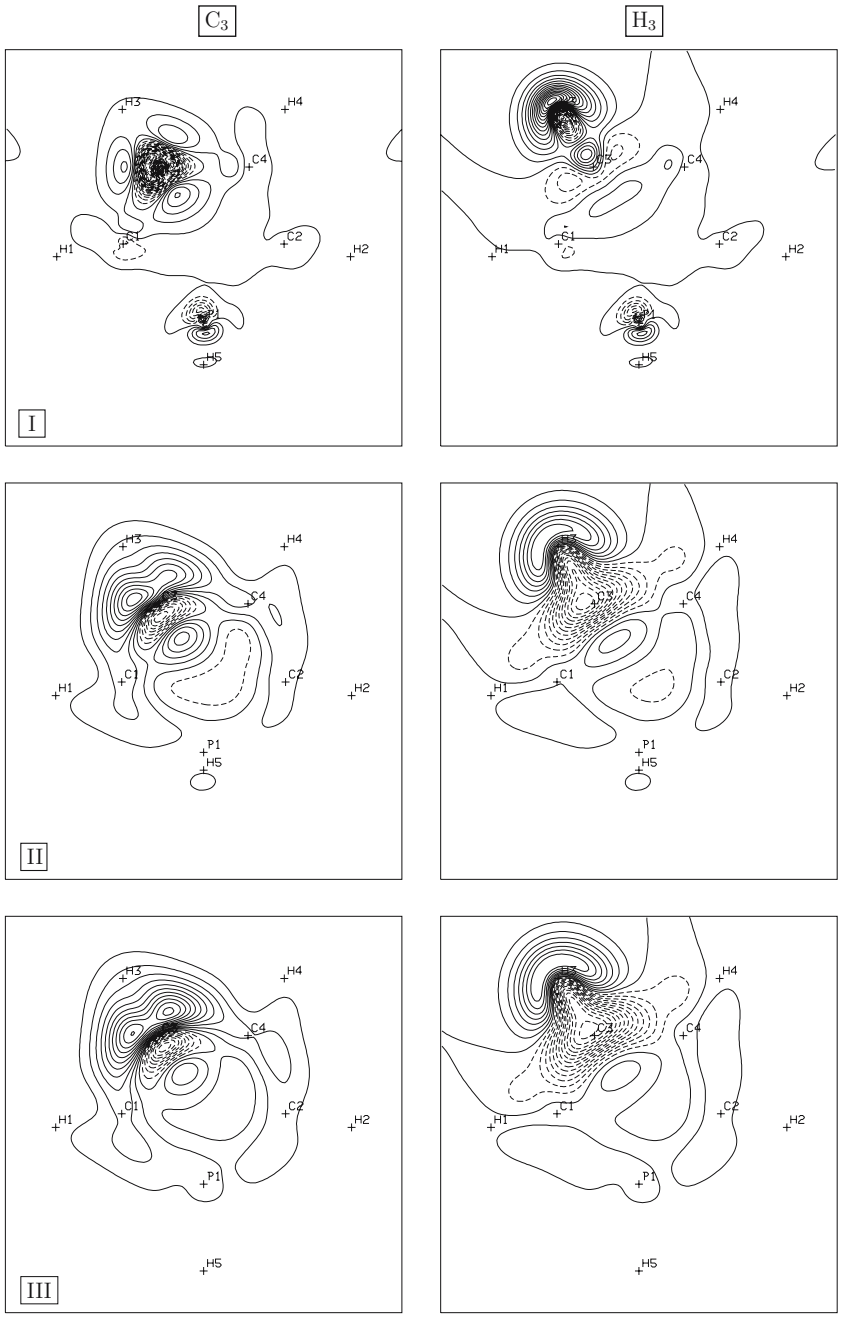

Fig. 6 The out-of-plane shielding density at hydrogen and carbon nuclei of phosphole induced by a magnetic field in the x direction. The plot planes are the same as in Fig. 2. The contours are associated with constant magnitude and are drawn in steps of 2×10^{-3} and 1×10^{-3} au for C and H, respectively

5 π distortivity and ring currents

It is generally held that the geometry of aromatics results from a balance between two contrasting mechanisms, the former, governed by σ electrons, tends to produce stiff planar structures with equal, or nearly equal, bond lengths, the latter, promoted by π electrons, favours bond alternation and deviation from planarity [21].

In benzene, the archetypal aromatic system, the π distortivity that would lead to a D_{3h} geometry with more localized C=C bonds, corresponding to the Kekulé structure, is overcome by the opposite tendency of σ electrons, driving planarization of the molecular framework. This is also the case of C_4H_4X five-membered ring heterocycles, with X=CH_2, NH, O, and S, in which the σ electrons win the energy-geometry competition determining planar ring structures and diatropicity sustained by π-electrons [36].

On the other hand, the real C_4H_4PH and C_4H_4AsH molecules prefer a distorted geometry [10–16,18,19]. As

shown in Table 3, the difference between C−C bond lengths tends to diminish by imposing an artificial planarity: the C_1–C_3 (C_3–C_4) distance increases (decreases) by ≈0.03 (0.04) Å passing from relaxed I to planar II and III geometries. Bond equalisation, typical of aromatics, is accompanied by energetic destabilization in these five-membered ring heterocycles.

In fact, the SCF and the B3LYP-DFT energies $W^{(0)}$ of the molecules in the absence of perturbation reported in Table 3 show that stability decreases by increasing planarity of the molecular structure. The aromatic stabilisation provided by π delocalisation, rationalised by various measures [42], is overcome in C_4H_4AsH and C_4H_4PH by the larger stabilisation achieved via ring distortion. Moreover, the results in Table 3 indicate that higher energetic instability is accompanied by increased mobility of the π electrons in a magnetic field and onset of more intense ring currents in C_4H_4AsH and C_4H_4PH. A smaller degree of electronic stability comes together with higher diatropicity, documented in the series I–III by the increase of $|\mathbf{J}|$ and by the magnetic quantifiers $\chi_{\parallel}$, $\sigma_{\parallel}^{H}$, and $\sigma_{\parallel}^{C}$.

These results for C_4H_4AsH and C_4H_4PH document inconsistencies among different aromaticity criteria [2,43], providing further evidence of strong discrepancies between energetic and magnetic descriptors, previously observed in bis-heteropentalenes [3,5] and in tetraazanaphthalenes [9].

6 Conclusions

Magnetic criteria yield quantitative descriptors of relative diatropicity in bent, partially, and fully planarized C_4H_4AsH and C_4H_4PH. The out-of-plane component of magnetic tensors, susceptibility and shielding at hydrogen and carbon nuclei, can be used to obtain a scale of magnetic aromaticity. The intensity of the ring currents induced in C_4H_4AsH and C_4H_4PH by a magnetic field normal to the plane of four C atoms increases by flattening the molecules. The stronger diatropicity of planar structures, shown by current density maps, shielding density maps, and magnetic indicators, is accompanied by higher energetic instability related to the distortivity of the π electrons. Therefore, the special mobility of the π electrons and the onset of ring currents in a magnetic field are related to molecular energetic instability.

Acknowledgments Support from the European research and training network "Understanding Nanomaterials from a Quantum Perspective (NANOQUANT)", contract No. MRTN-CT-2003-506842, and from the Italian MURST via PRIN funds, is gratefully acknowledged.

References

1. von Ragué Schleyer R (2001) Chem Rev 101:1115 and articles therein.
2. Cyrañski M, Krygowski TM, Katrizky AR, von Ragué Schleyer P(2002) J Org Chem 67:1333
3. Subramanian G, von Ragué Schleyer P, Jiao H(1996) Angew Chem Int Ed Engl 35:2638
4. Lazzeretti P(2000) Ring currents. In: Progress in nuclear magnetic resonance spectroscopy, vol. 36. Emsley JW, Feeney J, Sutcliffe LH (eds) Elsevier, Amsterdam, pp. 1–88
5. Cuesta IG, Jartín RS, Sànchez de Merás A, Lazzeretti P (2003) J Chem Phys 119:5518
6. Cuesta IG, Jartín RS, Sànchez de Merás A, Lazzeretti P (2004) J Chem Phys 120:6542
7. Cuesta IG, Jartín RS, Sànchez de Merás A, Lazzeretti P (2005) Mol Phys 120:789
8. Cuesta IG, Sànchez de Merás A, Lazzeretti P (2006) J Comput Chem 27:344
9. Cuesta IG, Sànchez de Merás A, Lazzeretti P (2006) J Comput Chem 27:1980
10. Egan W, Tang R, Zon G, Mislow K (1971) J Am Chem Soc 93:6205
11. Andose JD, Rauk A, Mislow K (1974) J Am Chem Soc 22:6904
12. Nyulászi L (1995) J Phys Chem 99:586
13. Dransfeld A, Nyulászi L, Schleyer PvR (1998) Inorg Chem 37:4413
14. Johansson MP, Jusélius J (2005) Lett Org Chem 2:469
15. Nyulászi L, Keglevich G, Quin LD (1996) J Org Chem 61:7808
16. Keglevich G, Böcskei Z, Keseru GM, Ujszaszy K, Quin LD (1997) J Am Chem Soc 119:5095
17. Cloke FGN, Hitchcock PB, Hunnable P, Nixon JF, Nyulászi L, Niecke E, Thelen V (1998) Angew Chem Int Ed Engl 37:1083
18. Nyulászi L (2001) Chem Rev 101:1229
19. Nyulászi L(2000) Tetrahedron 56:79
20. Lazzeretti P (2004) Phys Chem Chem Phys 6:217
21. Jug K, Hiberty PC, Shaik S (2001) Chem Rev 101:1477
22. Havenith RWA, Jenneskens LW, Fowler PW, Steiner E (2003) Chem Comm 748
23. Havenith RWA, Fowler PW, Jenneskens LW, Steiner E (2003) J Phys Chem A 107:1867
24. Frisch MJ, Trucks GW, Schlegel HB, Scuseria GE, Robb MA, Cheeseman JR, Zakrzewski VG, Montgomery JA, Jr, Stratmann RE, Burant JC, Dapprich S, Millam JM, Daniels AD, Kudin KN, Strain MC, Farkas O, Tomasi J, Barone J, Cossi M, Cammi R, Mennucci B, Pomelli C, Adamo C, Clifford S, Ochterski J, Petersson GA, Ayala PY, Cui Q, Morokuma K, Malick DK, Rabuck AD, Raghavachari K, Foresman JB, Cioslowski J, Ortiz JV, Baboul AG, Stefanov BB, Liu G, Liashenko A, Piskorz P, Komaromi I, Gomperts R, Martin RL, Fox DJ, Keith T, Al-Laham MA, Peng CY, Nanayakkara A, Gonzalez C, Challacombe M, Gill PMW, Johnson BG, Chen W, Wong MW, Andres JL, Head-Gordon M, Replogle ES, Pople JA(1998) Gaussian 98, Revision A.7. Gaussian, Inc., Pittsburgh
25. Zanasi R (1996) J Chem Phys 105:1460
26. Lazzeretti P, Malagoli M, Zanasi R (1991) Technical report on project " sistemi informatici e calcolo parallelo", Research Report 1/67, CNR
27. van Duijneveldt FB (1971) Gaussian basis sets for the atoms H-Ne for use in molecular calculations, Research Report RJ 945 IBM
28. McLean AD, Chandler GS(1980) J Chem Phys 72:5639
29. Woon DE, Dunning TH, Jr (1993) J Chem Phys 98:1358

30. Angeli C, Bak KL, Bakken V, Christiansen O, Cimiraglia R, Coriani S, Dahle P, Dalskov EK, Enevoldsen T, Fernández B, Hättig C, Hald K, Halkier A, Heiberg H, Helgaker T, Hettema H, Jensen HJA, Jonsson D, Jørgensen P, Kirpekar S, Klopper W, Kobayashi R, Koch H, Ligabue A, Lutnaes OB, Mikkelsen KV, Norman P, Olsen J, Packer MJ, Pedersen TB, Rinkevicius Z, Rudberg E, Ruden TA, Ruud K, Salek P, Sánchez de Merás A, Saue T, Sauer SPA, Schimmelpfennig B, Sylvester-Hvid KO, Taylor PR, Vahtras O, Wilson DJ, Ågren H, Dalton, An electronic structure program, Release 2.0, Dalton, (http://www.kjemi.uio.no/software/dalton/).
31. Pelloni S, Ligabue A, Lazzeretti P (2004) Org Lett 6:4451
32. Ferraro MB, Faglioni F, Ligabue A, Pelloni S, Lazzeretti P (2005) Magn Res Chem 43:316
33. Pelloni S, Faglioni F, Zanasi R, Lazzeretti P (2006) Phys Rev A 74:012506
34. The LINUX and WINDOWS versions of the graphic code used to obtain three-dimensional representations of the stagnation graph of arsole and phosphole molecules and the maps reporting streamlines and moduli of the current density are available as supporting information. This material can also be downloaded at https://theochem.chimfar.unimo.it/TCA/
35. Keith TA, Bader RFW (1993) J Chem Phys 99:3669
36. Pelloni S, Lazzeretti P Theor. Chem. Acc., (in press,) DOI:10.1007/s00214-006-0211-4
37. Ferraro MB, Lazzeretti P, Viglione RG, Zanasi R (2004) Chem Phys Lett 390:268
38. Gomes JANF (1983) J Chem Phys 78:4585
39. Gomes JANF (1983) Phys Rev A 28:559
40. Gomes JANF (1983) J Mol Struct (THEOCHEM) 93:111
41. Soncini A, Fowler PW, Lazzeretti P, Zanasi R (2005) Chem Phys Lett 401:164
42. Mo Y, von Ragué Schleyer P(2006) Chemistry Eur J 12:2009
43. Binsch G (1973) Naturwiss. 60:369